25th European Photovoltaic Solar Energy Conference and Exhibition /
5th World Conference on Photovoltaic Energy Conversion, 6-10 September 2010, Valencia, Spain

STATUS OF ULTRA-HIGH CONCENTRATOR MULTIJUNCTION SOLAR CELL DEVELOPMENT AT IES-UPM

Ignacio Rey-Stolle, Carlos Algora, Enrique Barrigón, Elisa García-Tabarés, Iván García, Pilar Espinet
Instituto de Energía Solar – Universidad Politécnica de Madrid (IES-UPM)
ETSI de Telecomunicación; Avda. Complutense 30; 28040 Madrid (Spain)
Phone: +34 91 4533552; Fax: +34 91 5446341; Email: irey@ies-def.upm.es

ABSTRACT: After the successful implementation of a record performing dual-junction solar cell at ultra high concentration, in this paper we present the optimization of key aspects in the transition to a triple-junction device, namely the heteronucleation of III-V structures onto germanium substrates. This optimization is based on in-situ RAS measurements during the MOVPE growth of the triple-junction solar cell structure and subsequent AFM analysis. The correlation between RAS and AFM allows detecting which RAS features correlate with good morphology and low RMS roughness. TEM analysis confirms that the quality of the triple-junction structures grown is good, revealing no trace of antiphase disorder, and showing flat, sharp and clear interfaces. Triple-junction solar cells manufactured on these structures have shown a peak efficiency of 36.2% at 700X, maintaining an efficiency over 35% from 300 to 1200 suns.
Keywords: III-V semiconductors, concentrator cells, multijunction solar cell

1 INTRODUCTION

A promising way to reduce levelised cost of photovoltaic electricity is the use of highly efficient solar cells at high concentrations [1]. In terms of cell efficiency, great progress has been made worldwide in the last years with record performing triple-junction solar cells based on III-V semiconductors with efficiencies over 40% [2-4]. However, this excellent peak efficiencies where always obtained at concentrations ranging from 150 to 400 suns; whilst our cost calculations show that the most advantageous concentration range to exploit such devices is ultra high concentration (UHCPV), namely, beyond 1000 suns. At this illumination, costs below 1€/W_p can be achieved for the whole PV plant [1]. After the successful implementation of a record performing dual-junction solar cell at high concentration [5], in this paper we present the optimization of key aspects in the transition to a triple-junction device and the results of the triple-junction solar cells manufactured.

2 SOLAR CELLS FOR UHCPV

Last year, our group presented a record-performing GaInP/GaAs dual-junction solar cell with a maximum efficiency of 32.6%, which remained virtually constant for concentrations ranging from 400 to 1000 suns [5]. Moreover, the efficiency didn't decrease steeply above 1000 suns but stayed above 30% up to concentrations higher than 3500 suns [5]. This device demonstrated that the attainment of high efficiencies at 1000 suns and above is a reachable goal. However, despite this excellent result it is clear that a dual-junction solar cell −though having interesting applications in approaches that aim substrate reuse, need substrate removal [6] or aim spectral splitting− has a limited efficiency potential when compared to state-of-the-art triple-junction solar cells. Accordingly, this methodology for UHCPV design is being applied to the development of lattice matched GaInP/GaInAs/Ge triple-junction devices, with the goal of achieving efficiencies in excess of 40% at 1000 suns and above.

Figure 1 compares the structures of the record dual-junction solar cell [5] and the current design of triple-junction solar cells under development at IES-UPM. It can be noticed that the transition to a triple-junction forces key changes in the device. The main modification is of course related to having to deal with a new substrate –a germanium wafer– which will act both as the mechanical support for the whole device as well as the third subcell. In addition, there are more subtle changes such as: (a) the need to modify the composition of virtually all the layers in the middle and top subcells to cope with the slight difference in lattice constant between Ge and GaAs; and (b) a second tunnel junction has to be added between the bottom and middle subcell, which has to be fine tuned to withstand the long thermal load associated to the growth of the middle and top subcell without degradation of the tunnelling characteristics.

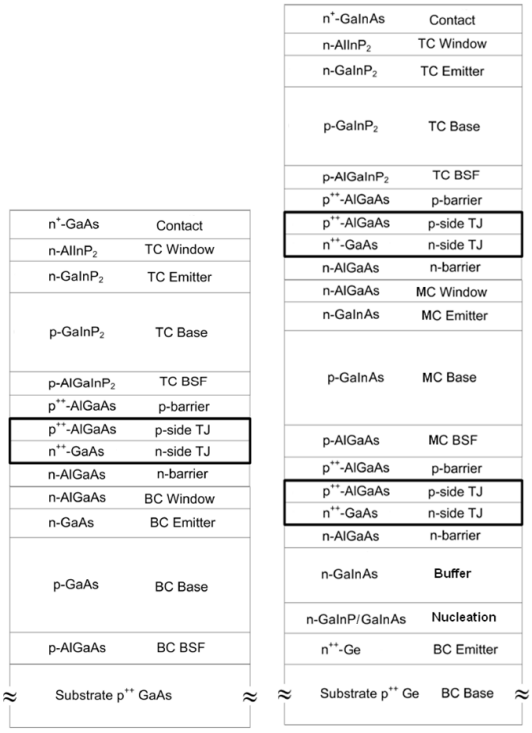

Figure 1: Comparison of dual and triple-junction solar cell semiconductor structures manufactured at IES-UPM

3 TRIPLE-JUNCTION GROWTH OPTIMISATION

A key task in the development of a multijunction solar cell on germanium is the optimization of the heteroepitaxial growth of III-V layers on this material. This has essentially two main requirements: (1) III-V epilayers on Ge have to provide a defect-free template for subsequent epitaxial growth; and (2) during the initial stages of III-V growth on Ge, diffusion of group-V atoms into the substrate has to form a third junction with the required characteristics for producing a high efficiency solar cell. The attainment of these two requisites is usually accomplished by the growth of two specific layers, namely, the nucleation layer grown at conditions which optimise the III-V/IV interface and the buffer layer grown at conditions that hinder the propagation of any crystallographic defect that might occur during the growth of the nucleation layer and thus provide an optimum template for further epitaxial growth. Nevertheless, it is well known that the growth of a polar III-V compound –such as GaAs or GaInP– on non-polar germanium typically gives rise to a variety of problems, such as of antiphase domains (APD), misfit dislocations, hillocks, uncontrolled etching, lack of charge neutrality across the heterointerface and diffusions from the layer into the substrate and vice versa. In summary, a lot of material science has to be put into this interface to build on it a high efficiency solar cell.

Thereby, to optimise the growth of III-V materials on germanium is of key interest to be able to monitor the surface processes that take place during the initial stages of the growth. Reflectance Anisotropy Spectroscopy (RAS) is an excellent tool for this purpose in a MOVPE environment where other electron-based techniques are not usable due to the lack of ultra-high vacuum. Essentially, RAS is a measure of the difference in reflectance of normally incident polarized light between two orthogonal crystal directions in the surface plane, normalized to the mean reflectance [7].

In figure 2 the absolute value of the reflectance anisotropy (RA) signal at 2.1 eV is presented for three different strategies for the growth of a GaInP nucleation layer on germanium (namely, samples A, B and C). The use of GaInP nucleation layers on germanium presents some advantages as compared to the use of (In)GaAs, particularly lower group-V element diffusion depths which allow the formation of shallower emitters in the bottom subcell. Sample A corresponds to the case when no intentional PH_3 anneal is applied on the sample before the growth of GaInP actually starts (i.e. the PH_3, TMGa and TMIn flows are opened at the same time); sample B represents the case when an anneal under PH_3 is performed prior to the growth with a moderate PH_3 partial pressure (0.7 mbar); while sample C represents the case of an anneal under PH_3 with a high partial pressure (2.8 mbar).

As figure 2 shows, for the three samples, the starting point for the RA signal of the Ge wafer is practically zero. Again for the three cases, when PH_3 is opened, a spike in the RA signal is observed. For sample A this spike occurs just when the GaInP growth starts, while for samples B and C it takes place 60 seconds before when the anneal under PH_3 starts. Apart from the location of the spike, this anneal does not change the RA signal of sample B (annealed under a low pressure of PH_3) as compared to sample A (no anneal under PH_3). This indicates that annealing under low flows of PH_3 does not seem to affect significantly the surface state of the germanium wafer which, in this case, is mostly induced by the uncontrolled desorption of species from the reactor walls and susceptor. On the other hand, for sample C annealed under a high flow of PH_3, a sudden increase in the level of the RA signal is measured (see inset in figure 2). Spectroscopic analyses performed at this point indicate that this change corresponds to 1x2 surface reconstruction induced by P adatoms, in agreement with the observations of other authors [8-9].

The moment when GaInP growth actually starts (i.e. the moment when TMGa and TMIn are opened) is marked in figure 2 with a vertical arrow. At this stage, the signal starts to oscillate, as the reflectance does (not shown) due to optical interference. The main difference observed between samples A to C is the magnitude and duration of the first oscillation of the RA signal. The peak of the second oscillation is virtually identical for the three cases.

From figure 2 we can infer that the RA signal is sensitive to changes in the nucleation and prenucleation conditions. However, directly from the RA signature is difficult to establish which sample is best. It seems that sample C should be better than A or B since evidence of a strong reconstruction (i.e. possibly single domain) has been found before the growth starts, which is known to be one of the key elements for APD-free nucleation [10]. Moreover, the presence of initial oscillations of high amplitude in the RA signal (as in samples A and B) has been correlated to poor morphology in other systems such as GaInP-AlGaInP [11]. Therefore, in order to clarify this, AFM scans were performed. In figure 3 the AFM scans of the GaInP layer of these three samples are shown. For each case, the image on the left shows the topography (all in the same scale), and the one on the right the amplitude. The RMS roughness value of samples A, B and C are 1.20 nm, 0.84 nm, 0.58 nm, respectively. Some holes can be seen in the scan of sample A, possibly indicating the seminal formation of antiphase domains. Evidence of step bunching is also noticeable in the AFM images of samples A and B. On the other hand, the surface of sample C looks quite smooth and uniform across the scanned area.

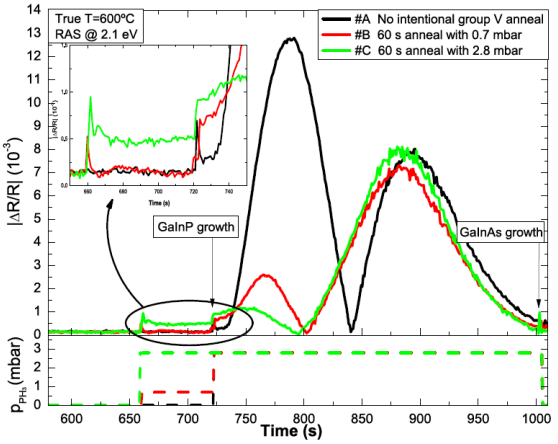

Figure 2: Time resolved RA signal at 2.1 eV for samples A, B and C (see details in the text). The lower part of the graph depicts the time evolution of the partial pressure of PH_3 for each sample.

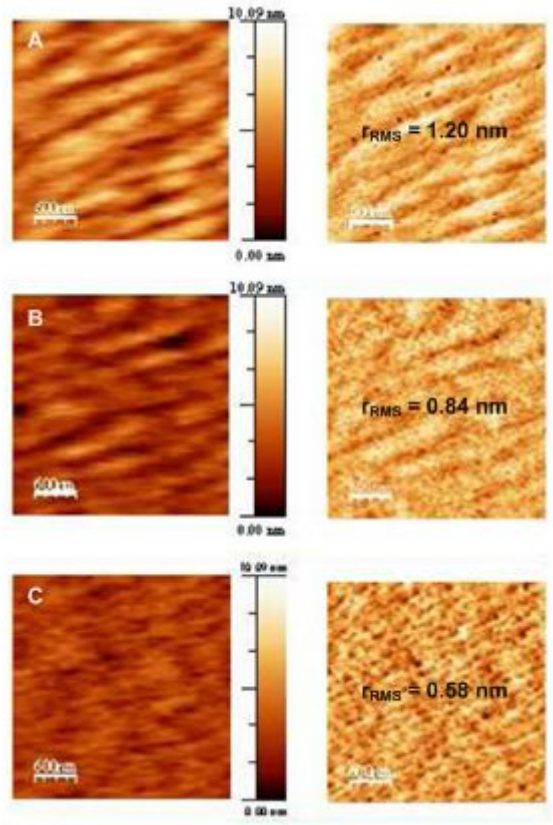

Figure 3: AFM scans of samples A, B and C. Images on the left correspond to topography and images on the right are amplitude. These images have been obtained with a Digital Instruments-Multimode IIIa microscope in tapping mode and have been processed using WSXM software [12]

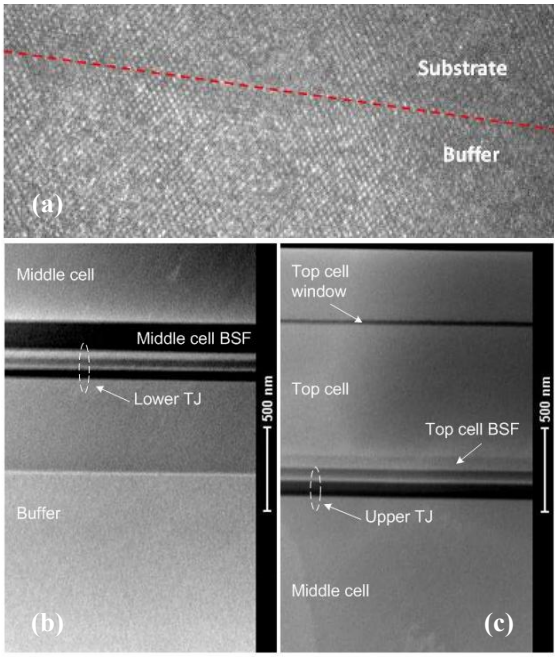

Figure 4: (a) High resolution TEM image of the Germanium/GaInP interface; (b) and (c) STEM images of the lower and upper parts of the triple-junction solar cell structure, respectively.

Triple-junction solar cells with the structure in figure 1 and the nucleation procedure of sample C were grown. In order to confirm the quality of the interface of sample C high resolution TEM images were taken on this sample. Figure 4.a shows one of these images where the interface is virtually indistinguishable (a red dotted line has been included as a guide-to-the-eye). No trace of APDs or APBs is observable in these images confirming the suitability of the nucleation procedure developed. On figures 4.b and 4.c STEM images of the lower and upper parts of the triple-junction solar cell structure are also shown. These figures show no trace of defects, with flat, sharp and clear interfaces, confirming the quality of the MOVPE process developed.

4 DEVICE RESULTS

The triple-junction solar cell structures were processed into 1 mm^2 high concentrator devices following a procedure very similar to that developed for our record dual-junction solar cell [5]. Figure 5 summarises the external quantum efficiency of these structures (EQE of Ge subcell not plotted for clarity). As shown in the figure, both curves virtually overlap (except at the bandgap edges due to differences in composition) indicating that the quality of minority carrier properties is very similar in both devices. The fitting of these curves suggests that the response in the top cell is somewhat low at the low wavelength range (300-500 nm) presumably due to the high doping of the emitter needed to keep the triple-junction solar cell series resistance low. On the other hand, the response in the top cell at its high wavelength range (500-700 nm) is absorption limited, indicating that minority carrier properties in the base are far from limiting the performance of the device. Regarding the (In)GaAs cell, its largest limitation is the loss of photocarriers absorbed in the GaAs cathode of the upper tunnel junction. The overall result is that the device is middle cell limited with a short circuit current of J_{SC} = 13.3 mA/cm^2 (AM1.5D ASTM G173 normalised to 1000 W/m^2), being the current in the top cell $J_{SC,TC}$ = 14.2 mA/cm^2.

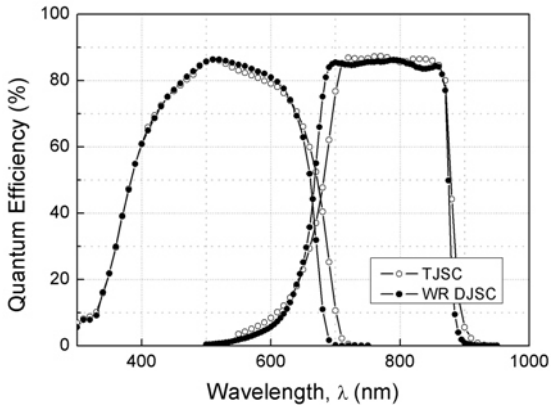

Figure 5: External quantum efficiency of dual (WR DJSC) and triple-junction solar cells (TJSC). Ge subcell EQE is not shown for clarity.

Figure 6 presents the concentrator results of the dual and triple-junction solar cells developed at IES-UPM. As this figure shows, for triple-junction solar cells efficiency is over 36% for concentrations between 550 and 850

suns, peaking at 700X with a 36.2%. After this maximum, the drop in efficiency is much steeper than in the case of the record dual-junction solar cell as a result of the rapid decrease of the fill factor after 500X. Preliminary investigations indicate that this behaviour is related to a incidental processing issue (front contact problem) as the new series resistance components associated to this structure (i.e. the germanium wafer and the additional tunnel junction) should only add minor contributions to the overall series resistance as compared to the dual-junction design.

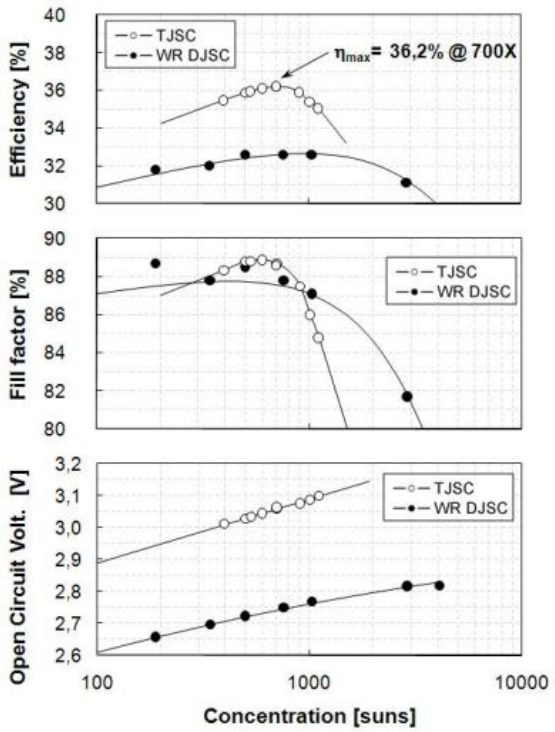

Figure 6: Concentration response of triple and dual-junction solar cells developed at IES-UPM

Simulations indicate that the way to raise the efficiency of this triple-junction solar cell is to implement a high bandgap cathode for the top tunnel junction and also a high bandgap top cell junction. The higher transmissivity of the tunnel junction would increase the short circuit current, and raising the bandgap of the GaInP in the top cell would also add up to the open circuit voltage. These two changes –provided that they do not add significant contributions to the series resistance– and a fine current matching between subcells, should bring efficiency above 40% at 1000X [1].

5 SUMMARY AND CONCLUSSIONS

Ultra High Concentrator PV (> 1000 suns) based on III-V multi-junction solar cells seems a robust strategy to decrease the cost of PV electricity. The design of high efficiency devices at such high concentrations presents multiple challenges. After the successful implementation of a record performing dual-junction solar cell at ultra high concentration, in this paper we have presented the optimisation of key aspects in the transition to a triple-junction device, namely the heteronucleation of III-V structures onto germanium substrates. This optimisation has been based on in-situ RAS measurements during MOVPE growth and subsequent AFM analysis, which allowed detecting which RAS features correlated with good morphology and low RMS roughness. TEM analysis confirms that the quality of the triple-junction structures grown by MOVPE is good, revealing no trace of APDs, and showing flat, sharp and clear interfaces. Triple-junction solar cells manufactured on these structures have shown a peak efficiency of 36.2% at 700X, with a value over 35% from 300 to 1200 suns. Simulations indicate that by implementing a high bandgap top cell and top tunnel junction, efficiencies of 40% at 1000X are reachable.

ACKNOWLEDGMENTS

This paper was supported by the Spanish *Ministerio de Ciencia e Innovación* under the CONSOLIDER-INGENIO 2010 program by means of the GENESIS FV project (CSD2006-004) and the research projects with references TEC2009-11143, TEC2008-01226 and PSS-440000-2009-30. The *Comunidad de Madrid* has also contributed under the NUMANCIA II Programme (S2009/ENE1477).

REFERENCES

[1] C. Algora, I. Rey-Stolle, I. García, B. Galiana, M. Baudrit, P. Espinet, E. Barrigón and J. R González, 34th IEEE PVSC, Philadelphia (USA), May 2009

[2] R. R. King, A. Boca, W. Hong, X.-Q. Liu, D. Bhusari, D. Larrabee, K. M. Edmondson, D. C. Law, C. M. Fetzer, S. Mesropian, and N. H. Karam, 24th European Photovoltaic Solar Energy Conference, Hamburg (Germany), September 2009

[3] W. Guter, J. Schöne, S. P. Philipps, M. Steiner, G. Siefer, A. Wekkeli, E. Welser, E. Oliva, A. W. Bett, and F. Dimroth, Appl. Phys. Lett. 94, 223504 (2009)

[4] J. F. Geisz, D. J. Friedman, J. S. Ward, A. Duda, W. J. Olavarria, T. E. Moriarty, J. T. Kiehl, M. J. Romero, A. G. Norman, and K. M. Jones, Appl. Phys. Lett. 93, 123505 (2008)

[5] I. García, I. Rey-Stolle, B. Galiana, and C. Algora, Appl. Phys. Lett. 94, 053509 (2009)

[6] J. Yoon, S. Jo, I. S. Chun, I. Jung, H-S Kim, M. Meitl, E. Menard, X. Li, J. J. Coleman, U. Paik, J. A. Rogers, Nature, Vol. 465, pp. 329–333 (2010)

[7] J.-T. Zettler, Progress in Crystal Growth and Characterization of Materials 35, pp. 27-98 (1997)

[8] J. Olson, W.E .McMahon, 2nd World Conf. on PV Solar Energy Conversion, Vienna (Austria) 1998

[9] N. A. Kalyuzhnyy, V. M. Lantratov, S. A. Mintairov, M. A. Mintairov, M. Z. Shvarts, N. K. Timoshina, V. Andreev, 23rd European Photovoltaic Solar Energy Conference, Valencia (Spain), September 2008

[10] L. Lazzarini, L. Nasi, G. Salviati, C. Z. Fregonara, Y. Li, L. J. Giling, C. Hardingham, D. B. Holt, Micron 31, pp.217-222 (2000)

[11] M. Zorn, M. Weyers, Journal of Crystal Growth 276, pp. 29-36 (2005)

[12] I. Horcas, R. Fernández, J. M. Gómez-Rodríguez, J. Colchero, J. Gómez-Herrero, A. M. Baro, Review of Scientific Instruments 78, 013705 (2007)